

<Constellation Mission>

Title: CubeSat-Constellation-Based Global Early Warning Tsunami Forecasting

Point of contact (POC): Kosuke Kanda¹

Email: csko21015@g.nihon-u.ac.jp

Co-authors: Masahiko Yamazaki¹, Tomoyuki Iida¹, Reiji Kobayashi¹, Kyogo Otani¹, Makoto Motoyama¹, Ryusuke Iwata¹, Kentaro Nakaizumi¹, Masashi Kamogawa²

Organization: ¹Nihon University, Japan, ²University of Shizuoka, Japan

Need

According to a study by the United Nations Office for Disaster Risk Reduction (UNDRR) [1], approximately 1.35 million deaths occurred due to natural disasters worldwide in the last 20 years. Of these deaths, 750,000 were caused by tsunamis. As an example, the 2011 Tohoku earthquake off the Pacific coast of Japan (Tohoku EQ) resulted in the deaths of approximately 20,000 people, primarily caused by the ensuing tsunami. According to a report by the Japan Meteorological Agency (JMA) [2], the tsunami forecast for the Tohoku EQ underestimated the magnitude (M) of the earthquake due to technical limitations. Consequently, the initial tsunami report underestimated the height of the tsunami at 3 m, while the actual maximum height reached 6 m [3,4]. This discrepancy is considered one of the reasons for the increased damage. The initial tsunami prediction report by the JMA relied on a database of numerical results obtained from tsunami propagation simulations conducted under various scenarios considering multiple magnitudes and all possible epicenters. The Tohoku EQ exemplified that magnitude determination using seismic waves reached saturation at M8. Consequently, tsunami forecasts tended to underestimate the impact of large earthquakes exceeding M8, resulting in increased damage. Today, there are three major types of early tsunami warning methods, including the one described above. This particular method allows for the initial report to be issued within a few minutes of the earthquake using only the epicenter and magnitude data. However, its accuracy is relatively low, leading to an underestimation of tsunamis, particularly in the case of huge earthquakes exceeding M8, as described above. The second method involves using Green's law to predict tsunami heights at the coastline based on the initial offshore tsunami heights, which are estimated from data on the initial wave recorded by submarine hydrometers on submarine cables [5][6], GPS wave gauges, and tsunami buoys [7]. Although this method has a certain degree of accuracy and is effective for early warning purposes, it can only be applied to the first wave, making it difficult to utilize for subsequent waves that occur after the initial impact of the tsunami on the coast. The third method is the most accurate in terms of spatiotemporal tsunami height prediction. By utilizing the initial tsunami source obtained through observation as an initial condition for tsunami simulations, this method enables highly accurate and comprehensive predictions of tsunami height in time and space. Although this method is ideal, it has not been widely employed for a long time because it is extremely difficult to determine the initial tsunami source through observation. In recent years, however, there has been an emerging possibility of achieving high-precision prediction by calculating the initial tsunami sources through inverse methods using observations from submarine cables, GPS wave gauges, etc. [8]. However, this method can be applied only to specific regions, such as the Pacific coast of Japan, where the required infrastructure is available.

Mission Objectives

For this mission, we construct a global early tsunami warning system that enables the most accurate forecast worldwide using a dense constellation of 6U CubeSats. The system is also able to predict tsunamis resulting from large earthquakes with magnitudes of 8 or greater. This is particularly significant, since such earthquakes can cause extensive damage, and the existing technologies have limited capabilities for accurate tsunami prediction in these scenarios. This system enables early tsunami forecasts in areas where submarine cables and dense global navigation satellite system (GNSS) buoys have not been installed. The satellite observations of the tsunami's current velocity and height and the phenomena caused by the initial tsunami source can be calculated using three methods by which the initial tsunami source is independently derived. Then, the resulting initial tsunami sources were optimized to obtain highly accurate initial conditions for high-precision simulations. For immediate forecasts, real-time data communication between each CubeSat and the ground station is essential.

Concept of Operations

The CubeSat estimates the propagating tsunami current velocity by analyzing signals from the Automatic Identification System (AIS) when ships at sea cross the tsunami [9]. Additionally, it calculates the propagating tsunami height using global navigation satellite system reflectometry (GNSS-R) [10], which is

based on observing the reflection of positioning signals transmitted by GNSS satellites off the tsunami. The CubeSat also estimates the initial tsunami source by observing the tsunami ionospheric hole (TIH) [11], which causes a decrease in the total electron content (TEC) in the ionosphere just above the initial tsunami source. This can be regarded as a quasi-direct observation method for the initial tsunami source. The conceptual diagram of the system is shown in Figure 1.

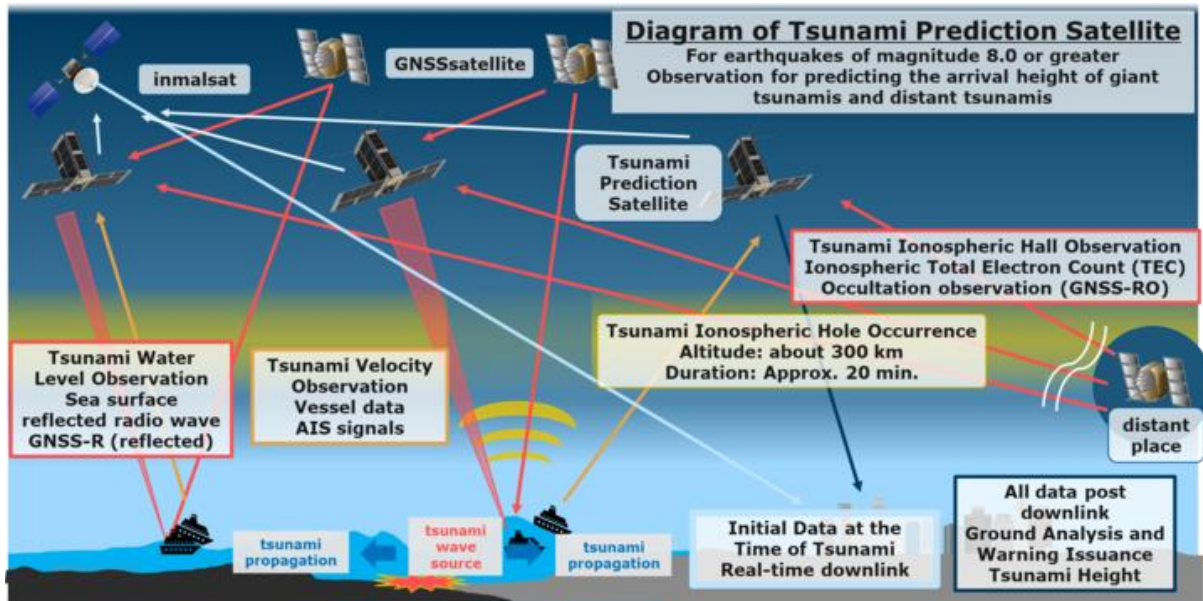


Figure 1. Conceptual diagram of the observation

1. Observation of propagating tsunamis from space
 - 1) Estimating the tsunami current velocity from ship speeds included in the AIS signal

The AIS is a system mandated for ships to have on board, consisting of a VHF transmitter that communicates with ground facilities or satellites. It transmits various information, such as the identification code, ship name, position, course, speed, and destination. The AIS is used to estimate the current velocity of a tsunami by analyzing data from ships that cross its path [9]. The difference between the ship's angle of motion, which is part of the ship information, and the actual angle of motion is extracted as the sine component and multiplied by the ship's speed to derive the ship's speed in the normal direction. The current velocity of the tsunami is subsequently obtained by approximating it to the velocity of the ship. Due to the approximately 2,500 km radius of the satellite footprint, a large amount of ship data can be acquired from the satellite. Since there are a large number of ships in the world's oceans, it is possible to calculate the propagating tsunami current velocity at many points.

- 2) Estimating tsunami heights using GNSS-R

GNSS-R is a method for estimating sea surface conditions by detecting sea surface reflected waves emitted from GNSS satellites at the altitudes of low Earth-orbiting (LEO) satellites [10]. The sea surface wind speed and sea surface wave height can be derived from the correlation between the sea surface slope and the sea surface wind speed. This correlation is calculated using the sea surface scattering coefficient, which indicates the roughness of the sea surface, from the delay-Doppler map (DDM). The DDM is based on the path difference between the direct signals received from the GNSS satellite and the signals reflected from the sea surface. To achieve a 20 cm height resolution for the observable tsunami height through GNSS-R, a constellation of 81 satellites distributed across 9 orbiting planes is required. This configuration enables the system to provide tsunami predictions within 15 minutes of the earthquake [10].

Both methods can measure the propagating tsunami current velocity and tsunami height. Using the multipoint observed values obtained through these methods, it becomes possible to perform inverse calculations and determine the initial tsunami source [8].

2. Quasi-direct observation of initial tsunami sources from space
 - 3) Estimating the initial tsunami source from the detection of the TIH using GNSS radio occultation (GNSS-RO)

GNSS-RO consists of a GNSS satellite serving as the source of the positioning signal and a LEO satellite acting as the GNSS receiver. This system calculates the TEC, which is the total number of electrons in a cylinder with a cross section of 1 m^2 along the radio propagation path between the receiver and the GNSS satellite. The TEC along the path is termed slant TEC (sTEC), and the value converted to the geocentric vertical direction is termed vertical TEC (vTEC). By using a large amount of sTEC data, the vertical distribution of the electron density at a certain latitude and longitude can be calculated. According to the literature, GNSS-RO observations are performed using 11 LEO satellites [12]; therefore, the spatiotemporal resolution of the electron density profile calculation is not high. In this project, however, we chose a sufficient number of CubeSats to enable dense observations and reproduce the TIH with high temporal resolution using GNSS-RO. In addition, to enhance the accuracy of the observation of the ionospheric electron density altitude profile, in situ electron density measurements were conducted using an impedance probe. Because the spatial variation of the TIH is highly correlated with the initial tsunami source, we used this relationship to estimate the initial tsunami source.

Key Performance Parameters

One key performance parameter is satellite lifetime. Our CubeSats are designed to work with the AIS and perform GNSS-RO and have a lifetime of 5 years. The number of CubeSats is another important key performance parameter. Because GNSS-R is the method required for the densest satellite constellation, we derived the number of satellites that can estimate the initial tsunami source through GNSS-R only. Since about 120 observation points are necessary to determine the initial tsunami source through inversion analysis, by conducting $10^\circ \times 10^\circ$ observations every second for a duration of 30 seconds, using a configuration of 15 orbital planes and 450 satellites, we

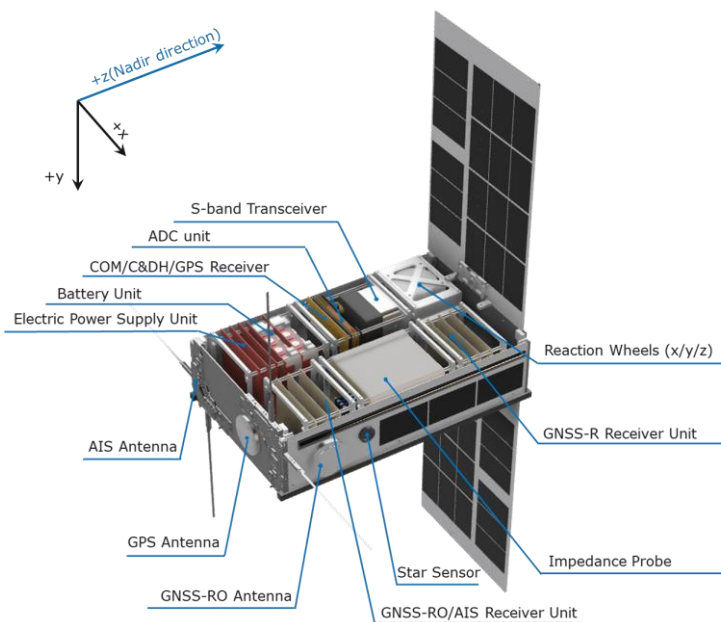


Figure 2. External view of the 6U CubeSat

can obtain a tsunami height accuracy of 20 cm. With this number of satellites, the AIS can cover a radius of approximately 800 km. For GNSS-RO, the comparison between FORMOSAT7 and other satellites [13] shows that the TIH can be measured with a temporal resolution of 30 s and a horizontal spatial resolution of 10 km. Real-time data downlink from CubeSats to ground stations is essential for early warning of tsunamis. For this purpose, CubeSats use the Inmarsat-based Inter-satellite Data Relay Service (IDRS) [14] to transmit tsunami current velocity, tsunami height, and GNSS-RO data to ground stations, with real-time onboard processing of spatiotemporal information enhancing the effectiveness of the system. Detailed housekeeping (HK) data for post-event analysis are then downlinked in the S-band. Pointing direction is yet another important performance parameter. Figure 2 shows that the AIS antennas, GNSS-R antennas, and other components in the $\pm Z$ plane perform geocentric pointing control for effective mission data acquisition.

Space Segment Description

The satellites are 6U CubeSats weighing 7.8 kg and measuring $366.0 \text{ mm} \times 226.2 \text{ mm} \times 100 \text{ mm}$ each at orbit insertion. After orbit insertion, the solar cells and the AIS antenna are deployed. The electrical power supply (EPS) provides power to each system, the command and data handling (CDH) system performs overall data control, and the attitude determination and control (ADC) system maintains attitude stability on three axes and the desired pointing directions for the communication antenna, AIS, and GNSS receiver. When a tsunami occurs, the communication (COM) system transfers the observation data acquired by the mission (MIS) system. An AIS and GNSS receiver are installed for each of the three missions. A three-axis attitude stabilization system was adopted for the satellites, with the Z axis pointing toward the center of the Earth, the Y axis in the direction of orbital progression, and the X axis orthogonal to the orbital plane. The satellite is equipped with IQ spacecom's [15] Xlink-S S-band transmitter/receiver and an S-band antenna and transmits GNSS-RO, TEC, and impedance probe data for data correction and HK data for satellite health status to PASCO's 7.4 m diameter ground station via S-band communication. A total of 172 MB of data / day

are transmitted at 2 Mbps. When the satellite determines that it is in the vicinity of a ground station, the attitude system performs ground station pointing control and communicates with the ground station for a maximum of approximately 10 minutes.

An Xlink-1 L-band transmitter and an IQ spacecom L-band antenna are also installed on the satellites. The 11.57 MB of tsunami parameter information (tsunami velocity, tsunami wave height, and GNSS-RO data) from the AIS, GNSS-R and GNSS-RO sent to the IDRS via L-band communication at a transmission rate of about 200 Kbps. Next, the data are downlinked from the IDRS to the ground in real time at a transmission rate of 432 Kbps. When the satellite receives data at the time of a tsunami, the ADC controls the pointing to the IDRS and communicates with the IDRS for a maximum of about 9 minutes. In Mission 1, the AIS data reception relies on the Satlab Polaris receiver [16], which can take into account the effects of Doppler shift and packet collision. The AIS transmitter/receiver antenna for 6U, provided by ISISPACE [17], is used to transmit and receive AIS signals. The GNSS receiver OEM7 from Amtex [18] and the TW3872E Embedded Dual Band Antenna from TALLYSMAN [19] are used to receive GNSS-R and GNSS-RO data for Missions 2 and 3. The receiver is configured to enable multipath reception for the reception of reflected waves.

The altitude of the satellite was set to 630 km, with a solar asynchronous orbit of 14 days. Through the power calculation, it was determined that to generate more power than the average consumption of 17.56 W for a single orbit of the satellite, two lithium-ion batteries with a nominal voltage of 3.7 V and a capacity of 4200 mAh were connected in series and in parallel. Additionally, a total of 120 NeXt Triple Junction (XTJ) solar cell from Spectrolab [20] are installed. These batteries had a depth of discharge of 15% and were confirmed to be capable of operating for five years.

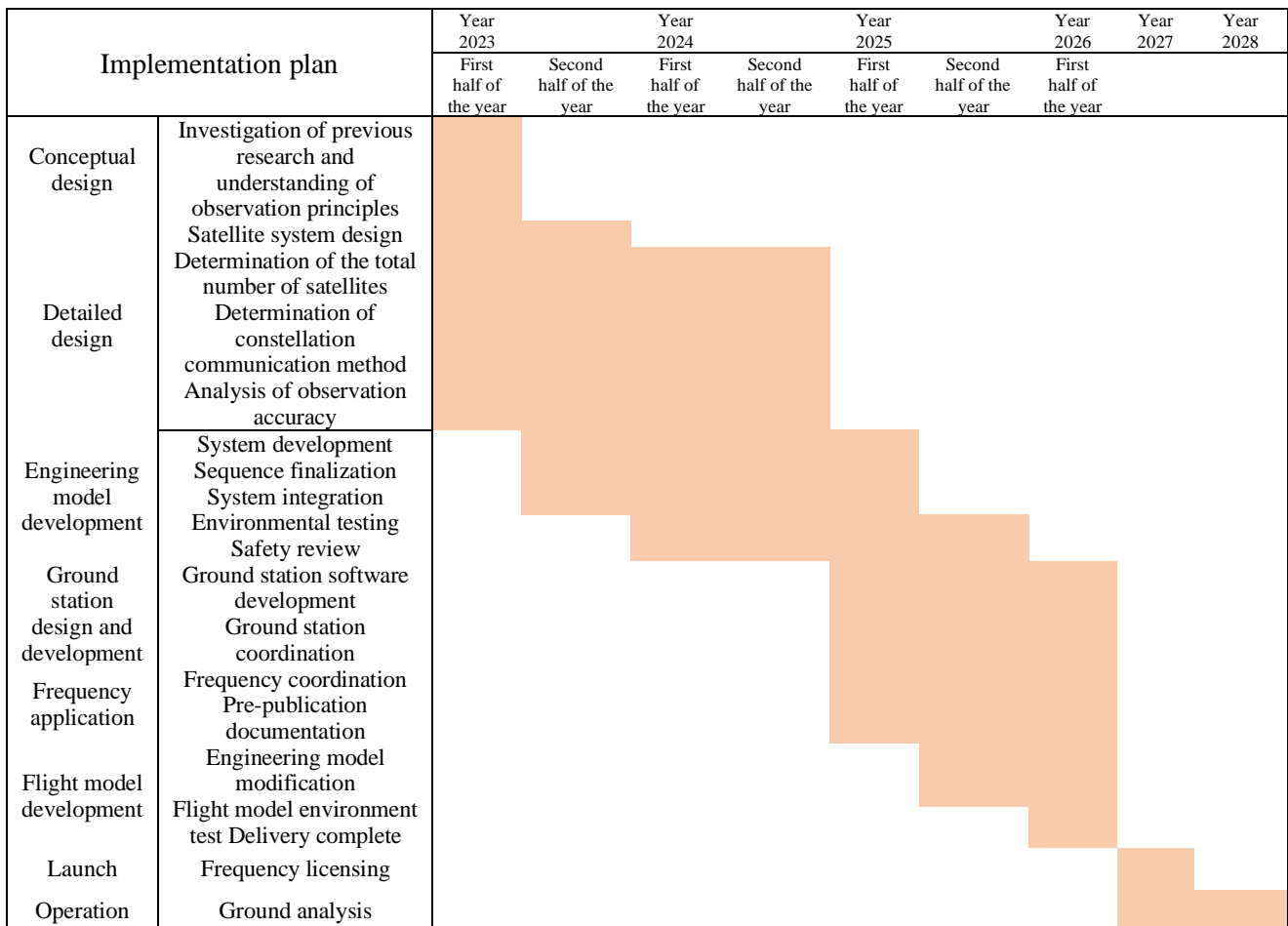


Figure 3. Implementation plan

Orbit and Constellation Description

A total of 450 CubeSats are required for the project, along with the corresponding orbits and constellation plans. The selected orbits are circular and positioned on a solar asynchronous orbit of $\pm 50^\circ$. This configuration allows observation of areas outside the polar regions with a low probability of tsunamis. Since the observation range of GNSS-R is set to $10^\circ \times 10^\circ$ in terms of the latitude and longitude of the earth, 15 orbits with different orbital inclination angles of 12° each were used. A feasibility analysis was conducted

using the orbit at 12 p.m. LTDN, which experience the most shading and impose the most stringent constraints on the amount of electricity generated. Regarding orbit injection, the CubeSats are injected into 15 orbital planes by rockets. Each rocket releases five CubeSats, resulting in a total of 90 rocket releases. The CubeSats are placed using differential drag disturbance [21] to ensure the proper spacing of the satellites.

Implementation Plan

The development of this CubeSat system is expected to take approximately three years, including system design, as shown in Figure 3. The development cost of one CubeSat is estimated to be approximately \$350,000, and the total cost of all CubeSats is approximately \$157.5 million. Assuming that each launched vehicle costs approximately \$7 million, the total cost for the entire fleet will be \$630 million, for a total cost of approximately \$787.5 million. Since all 450 CubeSats will be released by 90 rockets, 10 rocket launches are scheduled per month. The 450 CubeSats will be launched into space over approximately nine months, and satellite deployment will be completed in about one year after all CubeSats are released. The CubeSats will be deployed in the same orbit every four years to enable permanent observation.

References

- [1] Centre for Research on the Epidemiology of Disasters United Nations Office for Disaster Risk Reduction Tsunami Disaster Risk 2016: Past impacts and projections, 6p. (2016).
- [2] Central Disaster Management Council, Technical Survey Report on the Alarming of Disaster Lessons Learned, 76,122, (2010).
- [3] Japan Meteorological Agency, Overview of the 2011 Tohoku-Pacific Ocean Earthquake (in Japanese), JMA Technical Report, 133, (2012).
- [4] Japan Meteorological Agency, Method of tsunami forecast (in Japanese), <https://www.data.jma.go.jp/eqev/data/tsunami/ryoteki.html>, (accessed July 1, 2023)
- [5] National Research Institute for Earth Science and Disaster Resilience, Seafloor Observation Network for Earthquakes and Tsunamis along the Japan Trench: S-NET (in Japanese), <https://www.seafloor.bosai.go.jp/S-net/>, (accessed July 1, 2023)
- [6] Headquarters for Earthquake Research Promotion, Building Nankai Trough Seafloor Observation Network for Earthquakes and Tsunami (N-net) (in Japanese), <https://www.jishin.go.jp/main/seisaku/hokoku22b/k85-3-1.pdf>, (accessed July 1, 2023)
- [7] Y. Terada., Development of Tsunami and Wave Monitoring System using GPS Technology (in Japanese), J. Soc. Instrument Control Eng., 53, 6, (2014).
- [8] Y. Wang et al., Review on Recent Progress in Near-Field Tsunami Forecasting Using Offshore Tsunami Measurements: Source Inversion and Data Assimilation, Pure Applied Geophys., 178, 5109 (2021).
- [9] D. Inazu et al., Measuring offshore tsunami currents using ship navigation records, Prog. Earth Planetary Sci., 5, 38 (2018).
- [10] R. Stosius et al., The impact on tsunami detection from space using GNSS-reflectometry when combining GPS with GLONASS and Galileo, Adv. Space Res., 47, 843, 853 (2011).
- [11] M. Kamogawa et al., A possible space-based tsunami early warning system using observations of the tsunami ionospheric hole, Sci. Rep, 6, 37989 (2016).
- [12] Y. Xinan et al., Global 3-D ionospheric electron density reanalysis based on multisource data assimilation, J. Geophys. Res., 117, A09325 (2012).
- [13] R. Stosius et al., Simulation of space-borne tsunami detection using GNSS-Reflectometry applied to tsunamis in the Indian Ocean, Nat. Hazards Earth Syst. Sci, 10, 1359–1372 (2010).
- [14] IDRS, <https://www.idrsspace.com/technology>, (Acquired on June 10, 2023)
- [15] IQspacecom, <https://www.iq-spacecom.com/>, (Acquired on June 10, 2023)
- [16] satlab, Polaris 4-channel AIS Receiver, <https://www.satlab.com/products/polaris-ais/>, (accessed July 1, 2023)
- [17] ISISPACE, Antenna System for 6U/12U CubeSats <https://www.isispace.nl/product/antenna-system-for-6u-12u-cubesats/>, (Acquired on June 10, 2023)
- [18] AMTECS, High-precision GNSS engine OEM7, <https://www.amtechs.co.jp/product/gps/cat26/novatel/post-32.html>, (Acquired on June 10, 2023)
- [19] TALLYSMAN TW3872E Embedded Dual Band GNSS Antenna https://www.navtechgps.com/wp-content/uploads/TW3872E_DS.pdf, (Acquired on June 10, 2023)
- [20] SPECTROLAB, NEXT Triple Junction (XTJ), <https://www.spectrolab.com/DataSheets/cells/PV%20XTJ%20Cell%205-20-10.pdf>, (Acquired on June 10, 2023)
- [21] B.S. Kumar et al., Differential Drag as a Means of Spacecraft Formation Control, IEEE Trans. Aerospace Electron. Syst., 47, 2, (2011).